Ianalumab (VAY736) in primary Sjögren's syndrome: assessing disease activity using multi-modal ultrasound

T. Diekhoff[1], T. Fischer[1], Q. Schefer[2], M.G. Posch[2], T. Dörner[3], D. Laurent[4], Y. Li[4], F.D. Wagner[2], S.J. Oliver[4]

[1]*Institute for Radiology, Charité University Hospital, Berlin;*
[2]*Charité Research Organisation, Berlin;*
[3]*Department of Medicine/Rheumatology and Clinical Immunology, Charité University Hospital, Berlin, Germany;*
[4]*Novartis Pharma AG, Basel, Switzerland.*

Torsten Diekhoff, MD
Thomas Fischer, MD
Quirino Schefer, PhD
Maximilian Georg Posch, MD
Thomas Dörner, MD,
Didier Laurent, PhD
Yue Li
Frank D. Wagner, MD PhD
Stephen John Oliver, MD

Please address correspondence to:
Stephen John Oliver
Novartis Pharma AG,
Building WSJ386.11,
Novartis Campus,
4002 Basel, Switzerland.
E-mail: stephen.oliver@novartis.com

Received on September 15, 2020; accepted in revised form on September 23, 2020.

Clin Exp Rheumatol 2020; 38 (Suppl. 126): S228-S236.

Key words: Sjögren's syndrome, B cell depletion, salivary glands, ultrasonography, clinical trial

Funding: This study was funded by Novartis Pharma AG, Switzerland.

Competing interests: T. Diekhoff reports personal fees from Novartis outside the present work. T. Fischer has received honoraria from Canon Medical Systems for scientific talks at different congresses. D. Laurent, Y. Li and S.J. Oliver are full time employees of Novartis Pharma AG, Switzerland and own company stocks. T. Dörner has received scientific consulting fees from Novartis. The other authors have declared no competing interests.

ABSTRACT

Objective. *To apply serial ultrasound (US) assessments to show effects of ianalumab (anti-BAFF-R monoclonal antibody) on inflamed salivary glands of patients with primary Sjögren's syndrome (pSS).*

Methods. *In a single-centre, 24-week double-blind study (NCT02149420), 27 pSS patients of moderate-to-severe activity were randomly assigned to receive a single i.v. dose of either 3 mg/kg or 10 mg/kg ianalumab, or placebo. Concurrent with clinical and laboratory outcomes, multi-modal US images were acquired of bilateral parotid glands (PG) and submandibular glands (SMG) at weeks 0, 6, 12, and 24. Applied US modalities included 1) B-mode echostructure scored by de Vita classification, 2) macrovascular blood flow by power Doppler, and in PG only 3) microvascularisation using contrast-enhanced US (area under the curve, time to peak or TTP) and 4) gland stiffness by sonoelastography.*

Results. *Clinical study results were previously published. US data for PG differed from SMG but were comparable between respective left and right sides of these glands. Numerical improvements in salivary gland quality and declining tissue inflammation were observed in treated versus placebo groups, including more patients achieving ≥1-point reduction from baseline in De Vita score, together with trends towards decreased perfusion and stiffness. Correlations between clinical endpoints and US parameters were largely restricted to microvascular perfusion TTP and at the 12-week timepoint when ianalumab effects were predicted at maximal.*

Conclusion. *Early in vivo signs of salivary gland improvement in response to an effective intervention can be shown without need of biopsy by using a non-invasive, comprehensive, ultrasound-based approach over multiple time points.*

Introduction

Primary Sjögren's syndrome (pSS) is an autoimmune disease characterised by marked mucosal dryness due to lymphoid infiltration and progressive destruction of exocrine glands, most prominently the salivary and lacrimal glands (1, 2). Additionally, systemic disease manifestations are often present, including disabling fatigue, diffuse musculoskeletal pain and, in a subset of patients, a heterogeneous range of organ-specific involvement.

Recent development and validation of pSS disease activity measures, including the physician-scored EULAR Sjögren's Syndrome Disease Activity Index (ESSDAI) (3, 4) and the patient-reported questionnaire EULAR Sjögren's Syndrome Patient Reported Index (ESSPRI) (5), have facilitated clinical trials in this patient population to test novel therapies (6-9). However, these assessments do not necessarily provide objective and quantifiable information on therapeutic responses within exocrine tissues directly targeted by the disease. Histological evaluation of salivary gland tissue is limited by variable focal involvement of these tissues and reluctance of patients to undergo serial biopsies.

Salivary gland ultrasound (SGUS) techniques, including B-mode, power Doppler, contrast-enhanced sonography (CEUS) and sonoelastography, provide additional, tissue-focused perspectives on pSS disease activity (10-14). In contrast to the inherent variability in measuring salivary flow, invasiveness of gland biopsies and radiation exposure associated with sialography and scintigraphy, SGUS is a readily available, repeatable, non-invasive, versatile modality to directly assess glandular structure, perfusion and mechanical tissue properties (15). Furthermore, pSS patient studies have shown good

correlations between SGUS-detected abnormalities and clinical, laboratory and histology findings (16-19). However, reports of SGUS evaluation within the context of randomised, controlled, clinical trials in pSS patients have been limited in number and only as smaller sub-studies (20-22).

B lymphocytes and B cell activating factor of the TNF family (BAFF) signalling are considered to have central roles in pSS pathogenesis (23). Ianalumab (VAY736) is a human IgG1/κ mAb against the BAFF-receptor (BAFF-R) that eliminates B cells via dual mechanisms-of-action, (i) enhanced, antibody-dependent, cellular cytotoxicity (ADCC), and (ii) induction of B cell apoptosis through BAFF:BAFF-R signalling blockade. A randomised, double-blind, placebo-controlled study of single dose ianalumab in pSS patients (24) recently demonstrated a trend of positive therapeutic effects across a range of clinical outcomes together with profound B cell depletion of long-lasting duration. In parallel, these study patients were also evaluated by SGUS at baseline and again at 6, 12 and 24 weeks using a comprehensive imaging protocol assessing glandular echostructure, macro- and micro-vascular flow, and tissue stiffness. Similar to the clinical findings, there was a trend of positive therapeutic effects over time across multiple SGUS parameters, thus demonstrating that early and objective signs of salivary gland improvement can be detected in randomised, placebo-controlled trials in the pSS disease population without resorting to serial biopsies.

Patients and methods

Study design, patients and clinical outcomes

This single centre, 24-week study (NCT0214920) was previously described (24). Briefly, the study was conducted between 23 May 2014 and 07 February 2018. Patients were randomly assigned in a blinded manner to receive a single i.v. infusion of placebo or VAY736 dosed at either 3 mg/kg or 10 mg/kg. Enrolled patients fulfilled revised American-European consensus criteria for pSS (25), were either seropositive for anti-SSA or required to have ANA ≥1:160 and be seropositive for rheumatoid factor, and to have a stimulated salivary flow rate of >0 mL/minute and show active disease (ESSDAI ≥6). Exclusion criteria included concurrent connective tissue diseases, prior use of any B-cell depleting therapy, or use of other biologics within 180 days prior randomisation. Permitted concomitant medications included hydroxychloroquine and/or methotrexate, provided that patients were previously on a stable dosing regimen. Clinical outcomes were measured blinded at baseline and at weeks 6, 12 and 24 as well as unblinded upon B cell recovery (end of study, EoS). These clinical outcomes included the ESSDAI (3, 4), the ESSPRI (5), Physician's Global Assessment (PHGA) and patient-reported outcomes for fatigue (Multi-dimensional Fatigue Index, MFI) (26) and general quality of life (Patient's Global Assessment, PTGA; Short Form-36, SF-36) (27). Additional outcomes measured only within the blinded study period included salivary flow rate (stimulated and non-stimulated) and Ocular Staining Score (OSS) (28). All patients provided written informed consent before study participation. Laboratory-based measures included circulating leucocyte subsets and markers of B cell activity. This research was carried out in compliance with the Helsinki Declaration, with protocol and informed consent approved by local ethics committee before study initiation (Nr. 13/0418-EK11, Ethik-Kommission des Landesamt für Gesundheit und Soziales Berlin).

Ultrasound assessments

Concurrently with other clinical and laboratory outcomes, ultrasound images were acquired at baseline and again at weeks 6, 12 and 24, with SGUS data available for all 27 enrolled patients at all 4 time points with some exceptions (see statistical analysis). The sonography was performed by one of two expert physicians in a structured fashion and under the same conditions for each patient at baseline and follow up. The operators were trained and standard slices determined in five test patients. The conductor of the sonography was at all times blinded to the patients' treatment. Patients were placed in the supine position with the neck hyperextended and head slightly turned to the side opposite the glands being examined. High resolution 2-D acquisitions were performed with a real time scanner (Aplio 500, Toshiba, Japan) equipped with a 5–14 MHz broadband linear transducer (PLT-1005BT). The 9-14 MHz frequency range linear transducer was used to characterise and measure the size of parotid glands (PG) and submandibular glands (SMG) from B-mode images, assess gland macro-vascularisation from power Doppler and, by applying the real-time sono-elastography mode also embedded in the scanner (SElasto), measure PG stiffness. The 5 MHz was used to measure blood flow changes from microvascularisation of the PG by means of contrast enhancement. The PG was examined in an oblique-coronal (longitudinal) plane; the SMG in oblique-sagittal (longitudinal) orientation.

- *B-mode PG and SMG thickness and staging*. Disease staging was performed according to the following parameters: parenchymal homogeneity, echogenicity, thickness (mm) of the glands and posterior border. Results were evaluated, and classification scoring ranging from 0 to 4, denoting increasing disease severity, was assigned (10, 29). Patients whose score had at least a one-point reduction from baseline were designated De Vita responders.
- *Power Doppler.* PG and SMG images were obtained with at least one image in longitudinal orientation. Vascularisation pixels within a region of interest were automatically quantified by software and expressed as the area of vascular spots (%) within a defined window of 15 mm x 10 mm.
- *Contrast-enhanced ultrasound*. Continuous SGUS after contrast injection was performed using the dedicated technique of harmonic imaging at a low mechanical index (<0.1) and a low tissue signal (AP 0.1%). Using this technique, the signal emitted by micro-bubbles was followed over time. To this end, a 2.4 ml injection of contrast agent (sodium hexafluo-

ride bubbles; SonoVue, Bracco Diagnostics, Inc., NL) was administered within 4 seconds followed by a 5 ml saline flush. The arterial inflows of contrast medium and parenchymal phase were digitally recorded over 30 seconds. This procedure was repeated once per session. The time inflow curve was generated from raw data and analysed using the ultrasound device built-in tool (TIC software). Regions of interest were placed on the PG and estimates of contrast agent influx calculated by time to peak (TTP in seconds) and area under the curve (AUC).

- *Sonoelastography of the parotid gland*. Sonoelastography with real-time analysis was used to measure PG stiffness, a tissue characteristic affected by pSS (30). Transducer pressure resulting in an optimal image was determined previously (31, 32). Changes in tissue elasticity were depicted using sonoelastography with single-shot technique. The shear wave velocity and tissue stiffness (kilo-Pascals; kPa) were measured using a circular region of interest in representative tissue without artifacts.

The entire, above described, multimodal SGUS assessment took 10-15 minutes per patient.

Clinical assessments of exocrine gland activity

- *Salivary flow rate*. Patients were instructed not to eat, drink or smoke for 90 minutes before assessment of salivary flow. All assessments were performed at a fixed time of day to minimise fluctuations related to circadian rhythm. Unstimulated and stimulated salivary secretions were collected over 5 minutes using saliva collection aids according to manufacturer's instructions (Salimetrics, USA).
- *Ocular Staining Score* (28). In brief, slit lamp exam of each cornea under sequential staining by fluorescein and lissamine green dyes were objectively graded according to number of scored dots in defined conjunctival regions, with a maximum score of 12 per eye.

Table I. Patient demographics and baseline clinical disease activity.

		Placebo n=9	Ianalumab 3 mg/kg n=6	Ianalumab 10mg/kg n=12
Age in years, median (range)		50.0 (28, 58)	49.0 (32, 56)	58.5 (25, 70)
Female, n (%)		7 (77.8)	5 (83.3)	11 (91.7)
Caucasian, n (%)		9 (100.0)	6 (100.0)	12 (100.0)
Autoantibody profile, n (%)	SSA	9 (100.0)	6 (100.0)	12 (100.0)
	SSB	9 (100.0)	6 (100.0)	11 (91.7)
	ANA ≥1:80	8 (88.9)	6 (100.0)	12 (100.0)
	RF	5 (55.6)	5 (83.3)	10 (83.3)
Baseline ESSDAI, median (range)		10.0 (6, 19)	12.5 (6, 31)	10.0 (6, 18)
Baseline ESSPRI, median (range)		6.3 (3.0, 9.0)	6.3 (4.7, 7.7)	6.8 (3.0, 8.7)
Concomitant treatments**	CS*, n (%)	2 (22.2)	3 (50.0)	3 (25.5)
	[median dose; range]	[5.0; 5.0, 5.0]	[5.0; 5.0, 7.5]	[2.5; 1.0, 9.0]
	HCQ*, n (%)	5 (55.6)	2 (33.3)	5 (41.7)

*CS: corticosteroid dose (milligrams prednisolone or equivalent); HCQ: hydroxychloroquine.
**One patient (placebo arm) was enrolled on stable regimen of methotrexate.

Statistical analyses

The primary analysis for change from baseline in ESSDAI over the 24-week period of double-blind treatment was conducted via Bayesian repeated measures model, and the outcome was evaluated against predefined efficacy criteria (24). Repeated measurement models were also applied to change from baseline in other clinical endpoints including ESSPRI, MFI individual domains, PHGA and others. Exploratory endpoints such as salivary flow rate and SGUS data were summarised by treatment group and time and correlated with clinical endpoints. The two ianalumab dose groups were combined in the correlation analysis due to the limited sample size, and the Spearman correlation coefficient was used. The overall profiles of SGUS data differed greatly between PG and SMG but were comparable between an individual's respective left and right glands. Therefore, data for PG and SMG were analysed separately, with an individual's left and right glands averaged for group comparisons. In one patient lacking baseline SGUS data for the right PG, only left PG data were used for this time point. In addition, 2 patients (10 mg/kg VAY736) were missing SGUS data for Week 6, and 3 patients were missing SGUS data for Week 12 (3 mg/kg VAY736, n=2; 10 mg/kg VAY736, n=1).

Results

Main clinical and laboratory results

Clinical and laboratory results for this study were previously reported in detail (24). Briefly, 27 patients were enrolled and randomised as follows: 3 mg/kg ianalumab (n=6), 10 mg/kg ianalumab (n=12), placebo (n=9). All enrolled patients completed the initial, 24-week blinded period. Characteristics related to demographics and disease activity were comparable between treated and placebo study arms (Table I).

The primary outcome of change from baseline at Week 12 in ESSDAI between placebo- and ianalumab-treated patients, including the combined ianalumab group as well as the two individual dose groups, did not meet pre-defined criteria. However, similar trends showing a positive therapeutic effect by single dose ianalumab were observed across the primary outcome ESSDAI and all secondary clinical outcomes (ESSPRI, MFI, SF-36, global assessments by patient and physician) versus the placebo group. Differential response according to dosing group in the clinical outcomes was also observed. Early responses in patients receiving 3 mg/kg ianalumab tended to be transient and returned towards baseline levels by week 24 and EoS. Patients in the 10 mg/kg ianalumab group tended towards more sustained clinical responses up to Week 24 that also, except

Table II. Baseline SGUS modality values.

SGUS modality, mean (± SD)	Placebo	VAY736 (3 mg/kg)	VAY736 (10 mg/kg)
De Vita score			
Parotid	1.7 (1.35)	1.8 (0.84)	2.5 (0.81)
Submandibular	1.8 (1.03)	2.0 (1.26)	2.2 (0.72)
Gland thickness (mm)			
Parotid	20.28 (2.647)	17.60 (1.981)	19.38 (3.120)
Submandibular	13.69 (1.926)	13.08 (1.393)	12.71 (1.339)
Vascularisation index (%)			
Parotid	12.667 (15.1616)	14.620 (16.9513)	13.704 (10.2621)
Submandibular	18.588 (14.4865)	18.908 (10.7341)	20.625 (11.0358)
Parotid microvascular flow			
AUC (arbitrary units; a.u.)	135.178 (81.4470)	126.020 (78.6550)	143.325 (178.1472)
TTP (sec)	3.588 (0.7706)	3.534 (0.9102)	3.864 (0.9015)
Parotid stiffness (Kpa)	43.60 (16.493)	41.73 (19.663)	49.42 (19.567)

for SF-36, extended out to EoS. These observations were in accordance with the observed ianalumab exposure, *i.e.* ianalumab quantifiable levels detected approximately up to 8–12 weeks and to 12–16 weeks for the 3 mg/kg and 10 mg/kg dose groups, respectively. All ianalumab-treated patients experienced rapid and profound depletion of circulating CD19+ B cells. Time to B cell recovery varied considerably between individual patients, with a median recovery time of 402 days (range 49–1,036 days) in the 3 mg/kg dose group and 224 days (range 64–304 days) in the 10 mg/kg dose group.

Ultrasound

There were no significant differences between the 3 treatment groups in baseline SGUS values for the different modalities (Table II).

- *Disease staging and gland thickness*. The number and proportion of De Vita responders (Fig. 1) for PG and SMG were higher in the VAY736 treatment groups at Week 12 (10 mg/kg) and Week 24 (3 mg/kg and 10 mg/kg) than in the placebo group, and for SMG higher also at the 6-week timepoint. In contrast, there was no discernible change in gland thickness in ianalumab-treated groups compared to the placebo arm, with high variability observed within both treatment groups (Fig. 2A, 2B). Interestingly, maximum reduction from baseline for gland thickness appears to occur in the high dose group at Week 12; a time point at which a single 10 mg/kg infusion of ianalumab is predicted to still retain >90% receptor occupancy within tissues. Taken alone, these B-mode findings do not provide sufficient evidence of ianalumab treatment effect in pSS patients.

-*Large vessel blood flow*. The vascular index indicates abundance of blood flow by power Doppler sonography, and reductions from baseline would suggest less perfusion of swollen glandular tissues secondary to reduced inflammation. For both PG and SMG, changes from baseline for large-vessel blood flow were minimal for the combined VAY736 treatment group and for patients receiving placebo. When examined by treatment group (Fig. 2C, 2D), patients receiving the lower 3 mg/kg dose VAY736 had increased vascularisation at Week 6, persisting through to Week 24 in the SMG, while only transient increases were noted at 6 weeks in PG. Patients in the higher 10 mg/kg dose VAY736 treatment group experienced reductions of vascularisation index in PG and SMG at Week 12 and Week 24. Again, maximum reductions in large vessel blood flow appear to occur at Week 12 in the ianalumab high dose group.

-*Microvascularisation*. Contrast-enhanced evaluations were limited only to PG. Contrast agent influx measured by AUC indicates the total volume of perfusion over time. There was no change in AUC from baseline in any of the three groups, suggesting no differences in the overall, relative blood volume delivered to the PG tissues (Fig. 3A). The TTP parameter is inversely related to glandular tissue blood flow in which reduction in blood flow causes increased time needed for an i.v. bolus of SonoVue contrast to reach maximal

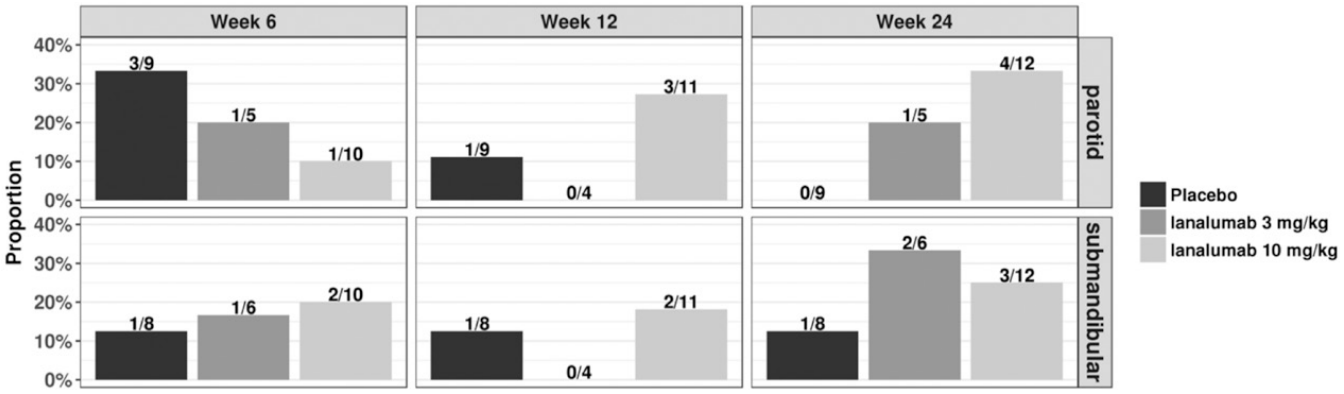

Fig. 1. Ianalumab effects on glandular echostructure (proportion of De Vita responders).
Responder is defined as attaining ≥1-point reduction from baseline. Mean baseline values for De Vita score in the three treatment groups are provided in Table II.

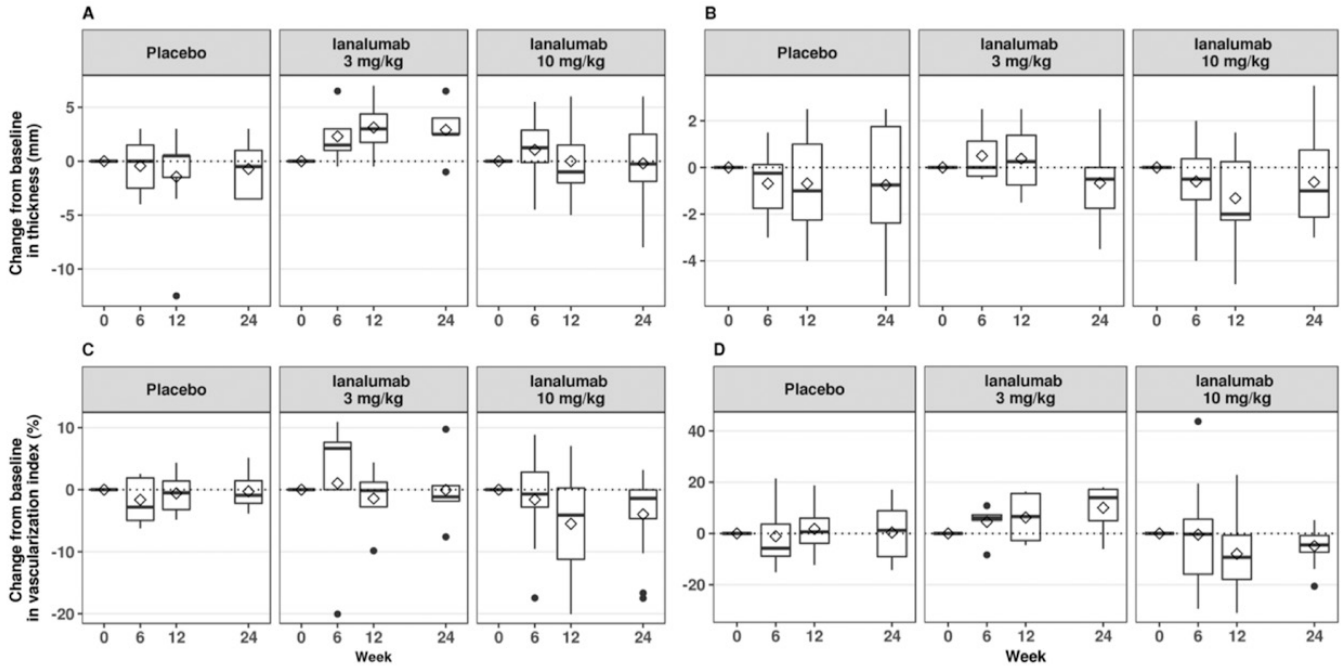

Fig. 2. Ianalumab effects on glandular thickness and large vessel blood flow.
Change from baseline absolute values are shown in boxplots with arithmetic means in diamond symbols of glandular thickness by B-mode for parotid (**A**) and for submandibular (**B**) glands, and for large vessel blood flow by power Doppler for parotid (**C**) and submandibular (**D**) glands. Mean baseline values of gland thickness and large vessel blood flow for the three treatment groups are provided in Table II. Dotted line denotes a change from baseline of zero, *i.e.* no difference from baseline.

intensity in passing through the microvasculature. In this study, TTP increased in patients receiving ianalumab 10 mg/kg compared to patients receiving 3 mg/kg ianalumab or placebo (Fig. 3B), thus inferring a lower degree of microvascularity in the higher dose group. Notably, the maximum effects upon microvascularisation occur over weeks 12–24 in the high dose group.

-Gland stiffness. Real-time elastography assessments were also limited to the PG. Compared to placebo, numerically greater reductions were observed in the low dose ianalumab group at weeks 12 and 24, and in the high dose group at weeks 6, 12 and 24 (Fig. 3C). Reductions in gland stiffness appeared to be maximally present at Week 12 in the high dose group.

-Correlations between SGUS parameters and clinical outcomes. Correlative analyses were performed on change from baseline for SGUS outcomes and of clinical disease measures at weeks 12 and 24 (Fig. 4A and B, respectively). The more significant clinical correlation trends are listed below together with Spearman coefficients and *p*-values:

1) Gland Thickness showed early direct correlation to Gland Stiffness at Week 12, becoming more significant by Week 24 (r=0.53, p=0.036). Gland Thickness inversely correlates with ESSDAI at Weeks 12 and 24 (r=-0.63, p=0.031; r=-0.45, p=0.056, respectively);

2) Large vessel blood flow (Vascular Index) correlated at Week 12 negatively with the Physician's Global Assessment (r=-0.44, p=0.018), and at Week 24 positively with the Ocular Staining Scores (Ocular-Left; r=0.48, p=0.0089);

3) Increased TTP (indicating reduced glandular micro-perfusion) correlated:

a) inversely to Ocular Staining Scores at Week 12 (Ocular-Right, r=-0.47, p=0.015; Ocular-Left, r=-0.57, p=0.0016), and at Week 24 (Ocular-Right, r=-0.49, p=0.013);

b) inversely to ESSPRI (r=-0.60, p=0.0076) at Week 24;

c) directly to PTGA (r=0.61, p=0.018) at Week 12;

d) inversely to unstimulated salivary flow (r=-0.4, p=0.014) at Week 12;

4) Gland Stiffness showed only weak correlations with clinical outcomes.

The Week 12 timepoint had a higher number of strong correlations between SGUS parameters and clinical outcomes compared to the Week 24 timepoint.

In addition, significant correlations were also found at Week 12 between SGUS modalities and the depletion of circulating CD19+ B cells by ianalumab, as defined by both the maximum depletion from baseline, and by the B cell count area under the curve (B cell AUC) measured over the 24-week treatment period, as follows:

a) Parotid gland thickness: maximum B cell depletion (r=-0.6, p=0.03); B cell AUC (r=0.59; p=0.04);

b) Parotid gland stiffness: maximum B cell depletion (r=-0.63, p=0.02); B cell AUC (r=0.57, p=0.04).

Discussion

In this study, direct SGUS assessment provided *in vivo*, tissue-level evidence of ianalumab effects in pSS patients. Proportionately more ianalumab-treated patients were staged as de Vita responders by B-mode assessment compared to placebo group. Moreover, SGUS assessments using dynamic contrast-enhancement and elastography

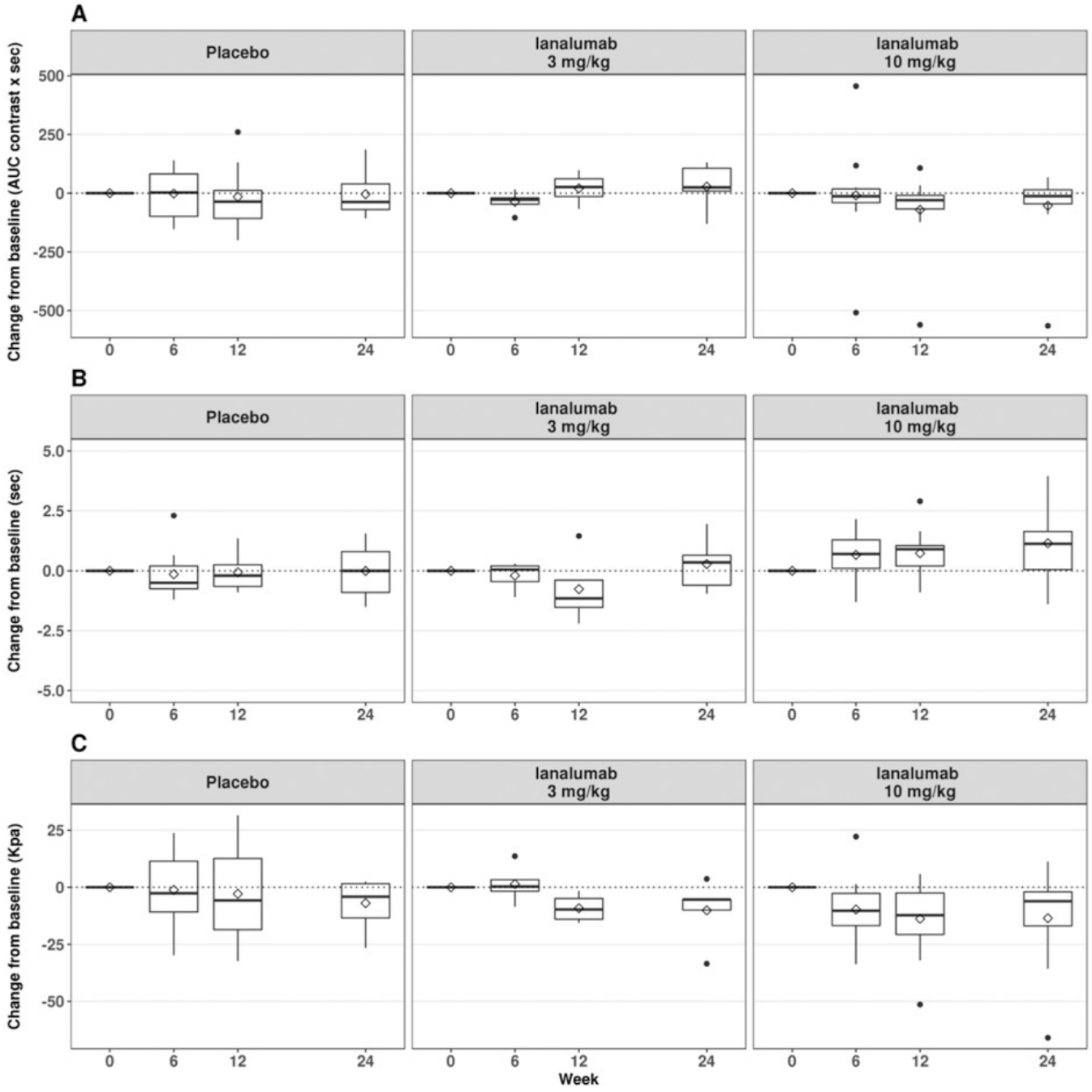

Fig. 3. Ianalumab effects on parotid glandular microvascular blood flow and stiffness.
Change from baseline absolute values are shown in boxplots with arithmetic means in diamond symbols for microvascular blood flow using CEUS by (**A**) AUC and by (**B**) TTP and for gland stiffness using elastography (**C**). Mean baseline values of AUC, TTP and gland stiffness for the three treatment groups are provided in Table II. Dotted line denotes a change from baseline of zero, *i.e.* no difference from baseline.

detected trends towards reduced levels of microvascularity and tissue stiffness in PG of patients receiving ianalumab, implying less inflammation and swelling. Correlations between SGUS findings and some clinical outcomes were also identified. Finally, all these parameters were completed for each patient within a relatively short time period and with a single device.

No single SGUS mode alone demonstrated clear evidence of beneficial effects by ianalumab over placebo. However, a consistent trend towards a therapeutic response was observed across the different SGUS modalities and time points, similar to clinical outcomes reported for this study (24). Moreover, SGUS-detected improvements were largely restricted to the higher ianalumab dose group and appeared maximal at Week 12, whereafter predicted ianalumab tissue levels from a single 10 mg/kg infusion would no longer support full BAFF receptor occupancy. Indeed, recently reported interim analysis results from an ongoing, dose-range finding study of monthly, subcutaneously-administered ianalumab in pSS patients (33) showed dose-dependent reductions

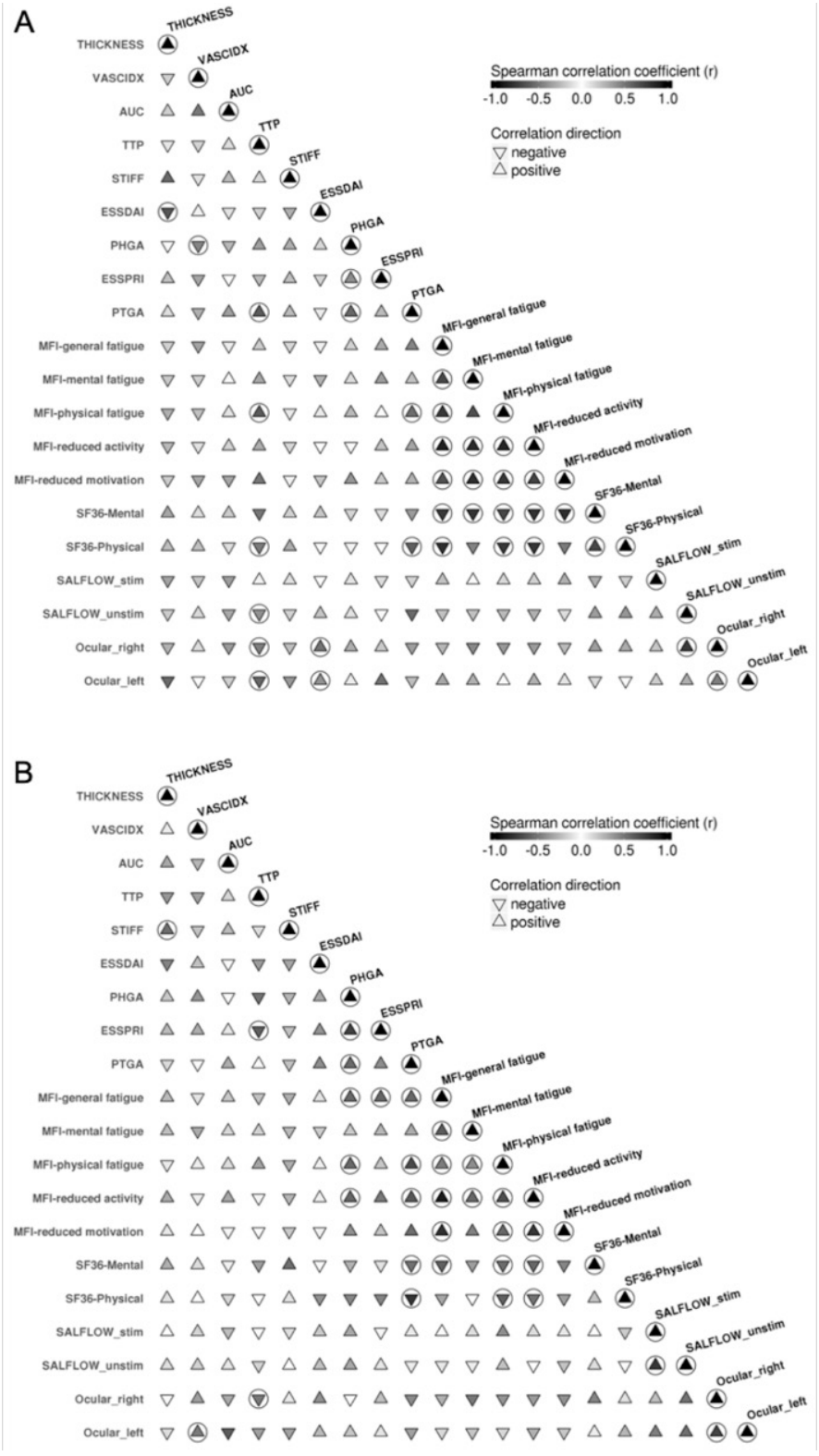

Fig. 4. Multi-modal SGUS correlations with observed clinical outcomes.
Correlations between the different outcomes in this study, measured by change from baseline at Week 12 (**A**) and Week 24 (**B**), with a focus on SGUS parameters *versus* clinical disease measures. Positive and negative correlations are indicated by triangles pointed up or down, respectively, with the darker the triangle, the stronger the correlation as determined by Spearman coefficient. Circled triangles indicate that the respective correlation is higher or equal to 0.4 and significant (p-value<0.05).
VASCIDX: vascular index; PHGA: physician global assessment; PTGA: patient global assessment; STIFF: gland stiffness; MFI-(components): multi-dimensional fatigue index; SALFLOW_stim: salivary flow stimulated; SALFOW_unstim: salivary flow unstimulated; OSS: ocular staining score.

of ESSDAI and increases in stimulated salivary flow over a 24-week period, with significant improvement over placebo limited to the high dose, 300 mg cohort for which systemic concentrations of ianalumab were predicted to provide sustained, full BAFF-R occupancy throughout this treatment period.
SGUS abnormalities appear to be reproducible and stable over at least one year (34) with evidence for reversibility with treatment, suggesting potential use as an efficacy outcome. However, reports are limited of SGUS application as an outcome in randomised, controlled trials. In the Tolerance and Efficacy of Rituximab in Primary Sjögren's Syndrome (TEARS) trial, a substudy of SGUS in 28 patients at a single site showed improved PG echostructure over placebo at 24 weeks in a significantly larger number of patients after a single rituximab cycle (20) along with correlations to the focus score and unstimulated salivary flow rate (21). The Trial of Anti-B cell Therapy in Patients with Primary Sjögren's Syndrome (TRACTISS) included a multi-centre, multi-observer substudy to compare the effects of rituximab *versus* placebo on SGUS evaluation by B-mode and power Doppler (22). Statistically significant improvements at weeks 16 and 48 were shown using an 11-point Total Ultrasound Score (TUS), albeit driven by changes in SG posterior border visibility and with no association found between TUS improvement and clinical outcomes.
Of the different US modalities tested in our study, elastography appeared most sensitive for detecting change in the ianalumab-treated patients versus patients receiving placebo. This technique is based on US-generated impulses passing through different tissue layers, with increased stiffness detected in glands containing oedema, lymphoid infiltrates, tissue damage and fibrosis. As such, elastography is less reliant on operator compression and generates absolute values without need for additional, subjective scoring; an advantage for use in clinical trials conducted across multiple study sites. Patients with pSS have been shown to have higher values of SMG elastography compared to

healthy controls as well as patients with SICCA (35, 36). Moreover, correlations were reported in pSS patients between elastography measurements and salivary gland function and histology as well as systemic disease as measured by ESSDAI, but not by ESSPRI (19, 37). In our study, elastography results were not strongly correlative with other SGUS parameters or with clinical outcomes but did show correlations with the breadth and depth of B cell depletion by ianalumab in these patients.

In this study, power Doppler and CEUS were used to visualise different elements of tissue perfusion, with power Doppler directly measuring blood flow velocity while CEUS visualising blood perfusion via small vessels through variables such as AUC and TTP. CEUS revealed trends towards reduction in microvasculature perfusion rates (*i.e.*, increased TTP) in both low and high dose ianalumab-treated patients, while power Doppler findings of numerical reductions in the macrovascular perfusion rate were limited to the high dose group only. TTP measurements by CEUS also generated the majority of stronger clinical correlations found for our ultrasound data. However, increased TTP was not consistently linked to improvement across the different clinical outcomes, and the significance was diminished by multiplicity. Also of note, these TTP clinical correlations were mainly limited to the 12-week timepoint when ianalumab effects were predicted to be maximal. Sensitivity of CEUS for detecting treatment response may be due to the less subjective measurement of perfusion kinetics using i.v. contrast compared to the more operator-dependent assessment of vascular flow by power Doppler. Previous CEUS reports have focused on diagnostic applications for differentiating benign glandular disease from malignant tumours (38-40). CEUS has also been reported to differentiate between patients with pSS and those with SICCA (41), with higher perfusion levels detected in the latter group. Thus, CEUS may be an attractive imaging modality for use in multi-centre clinical trials, albeit with the added challenges of invasiveness and potential for limited availability.

There are several limitations of the SGUS data obtained from our clinical study. This interventional trial was powered for clinical systemic disease outcomes, and the relatively low number of patients in each treatment group therefore limits statistical power for exploratory SGUS endpoints. Furthermore, the treatment period and ianalumab exposure may not have been of sufficient duration to adequately detect significant glandular changes by SGUS. Finally, salivary gland biopsy material was not available to collaborate the observed SGUS changes with histological changes of inflammatory cell infiltration and tissue structure.

In conclusion, early signs of salivary gland improvement in response to an effective intervention can be shown using a non-invasive, comprehensive, ultrasound-based approach applied at multiple time points without need of serial biopsies. Thus, SGUS is a non-invasive, rapid and relatively inexpensive means of providing *in vivo*, objective outcomes in target tissues (42). Although the exact significance of SGUS measurements for the underlying pSS disease is still being evaluated, SGUS can supplement the more established, clinical-based outcomes in early phase studies, potentially reducing the required sample size (43). For larger, multi-centre studies, a central reader is recommended to reduce intra/inter observer variability.

Acknowledgement

Fabriola La Gamba provided additional statistical support in preparation of this manuscript.

References

1. MARIETTE X, CHRISWELL LA: Primary Sjögren's syndrome. *N Engl J Med* 2018; 378: 931-9.
2. CAFARO G, CROIA C, ARGYROPOULOU OD *et al*.: One year in review 2019: Sjögren's syndrome. *Clin Exp Rheumatol* 2019; 37 (Suppl. 118): S3-15.
3. SEROR R, RAVAUD P, BOWMAN SJ *et al*: EULAR Sjögren's syndrome disease activity index: development of a consensus systemic disease activity index for primary Sjögren's syndrome. *Ann Rheum Dis* 2010; 69: 1103-9.
4. SEROR R, MARIETTE X, BOWMAN S *et al*: Accurate detection of changes in disease activity in primary Sjögren's syndrome by the European League against Rheumatism Sjögren's syndrome disease activity index. *Arthritis Care Res* 2010; 62: 551-8.
5. SEROR R, RAVAUD P, MARIETTE X *et al*.: EULAR Sjögren's syndrome patient reported index (ESSPRI): development of a consensus patient index for primary Sjögren's syndrome. *Ann Rheum Dis* 2011; 70: 968-72.
6. LIU X, LI X, LI X *et al*.: The efficacy and safety of total glucosides of peony in the treatment of primary Sjögren's syndrome: a multi-center, randomized, double-blinded, placebo-controlled clinical trial. *Clin Rheumatol* 2019; 38: 657-64.
7. CORNEC D, DEVAUCHELLE-PENSEC V, MARIETTE X *et al*.: Severe health-related quality of life impairment in active primary Sjögren's syndrome and patient-reported outcomes: data from a large therapeutic trial. *Arthritis Care Res* 2017; 69: 528-35.
8. MEINERS PM, ARENDS S, BROUWER E, SPIJKERVET FK, VISSINK A, BOOTSMA H: Responsiveness of disease activity indices ESSPRI and ESSDAI in patients with primary Sjögren's syndrome treated with rituximab. *Ann Rheum Dis* 2012; 71: 1297-302.
9. MEINERS PM, VISSINK A, KROESE FG *et al*.: Abatacept treatment reduces disease activity in early primary Sjögren's syndrome (open-label proof of concept ASAP study). *Ann Rheum Dis* 2014; 73: 1393-6.
10. JOUSSE-JOULIN S, DEVAUCHELLE-PENSEC V, MORVAN J *et al*.: Ultrasound assessment of salivary glands in patients with primary Sjögren's syndrome treated with rituximab: Quantitative and Doppler waveform analysis. *Biologics* 2007; 1: 311-9.
11. KOVACEVIC DO, FABIJANIC I: Sonographic diagnosis of parotid gland lesions: correlation with the results of sonographically guided fine-needle aspiration biopsy. *J Clin Ultrasound* 2010; 38: 294-8.
12. BURKE CJ, THOMAS RH, HOWLETT D: Imaging the major salivary glands. *Br J Oral Maxillofac Surg* 2011; 49: 261-9.
13. CAROTTI M, CIAPETTI A, JOUSSE-JOULIN S, SALAFFI F: Ultrasonography of the salivary glands: the role of grey-scale and colour/power Doppler. *Clin Exp Rheumatol* 2014; 32 (Suppl. 80): S61-70.
14. DAVID E, CANTISANI V, DE VINCENTIIS M *et al*.: Contrast-enhanced ultrasound in the evaluation of parotid gland lesions: an update of the literature. *Ultrasound* 2016; 24: 104-10.
15. BALDINI C, ZABOTTI A, FILIPOVIC N *et al*.: Imaging in primary Sjögren's syndrome: the "obsolete and the new". *Clin Exp Rheumatol* 2018; 36 (Suppl. 112): S215-21.
16. BALDINI C, LUCIANO N, TARANTINI G *et al*.: Salivary gland ultrasonography: a highly specific tool for the early diagnosis of primary Sjögren's syndrome. *Arthritis Res Ther* 2015; 17: 146.
17. LA PAGLIA GMC, SANCHEZ-PERNAUTE O, ALUNNO A *et al*.: Ultrasound salivary gland involvement in Sjögren's syndrome vs. other connective tissue diseases: is it autoantibody and gland dependent? *Clin Rheumatol* 2020; 39: 1207-15.
18. MILIC V, COLIC J, CIRKOVIC A, STANOJLOVIC S, DAMJANOV N: Disease activity and damage in patients with primary Sjögren's syndrome: prognostic value of salivary gland

ultrasound. *PLoS One* 2019; 14: e0226498.
19. CARABA A, BABALIC FC, IURCIUC S, IURCIUC M: The utility of major salivary gland ultrasonographic parameters in the diagnosis of Sjögren's syndrome. *Dis Markers* 2019; 2019:1716848.
20. JOUSSE-JOULIN S, DEVAUCHELLE-PENSEC V, CORNEC D *et al*.: Brief report: ultrasonographic assessment of salivary gland response to rituximab in primary Sjögren's syndrome. *Arthritis Rheum* 2015; 67: 1623-28.
21. CORNEC D, JOUSSE-JOULIN S, COSTA S *et al*.: High-grade salivary-gland involvement, assessed by histology or ultrasonography, is associated with a poor response to a single rituximab course in primary Sjögren's syndrome: data from the TEARS randomized trial. *PLoS One* 2016; 11: e0182787.
22. FISHER BA, EVERETT CC, ROUT J *et al*.: Effect of rituximab on a salivary gland ultrasound score in primary Sjögren's syndrome: results of the TRACTISS randomised, double-blind, multicenter substudy. *Ann Rheum Dis* 2018; 77: 412-16.
23. NOCTURNE G, MARIETTE X: B cells in the pathogenesis of primary Sjögren's syndrome. *Nat Rev Rheumatol* 2018; 14: 133-40.
24. DÖRNER T, POSCH MG, LI Y *et al*.: Treatment of primary Sjögren's syndrome with ianalumab (VAY736) targeting B cells by BAFF receptor blockade coupled with enhanced, antibody-dependent cellular cytotoxicity. *Ann Rheum Dis* 2019; 78: 641-47.
25. VITALI C, BOMBARDIERI S, JONSSON R *et al*.: Classification criteria for Sjögren's syndrome: a revised version of the European criteria proposed by the American-European consensus group. *Ann Rheum Dis* 2002; 61: 554-8.
26. SMETS EM, GARSSEN B, BONKE B, DE HAES JC: The multidimensional fatigue inventory (MF) psychometric qualities of an instrument to assess fatigue. *J Psychosom Res* 1995; 39: 315-25.
27. WARE JE, SHERBOURNE CD: The 36-item short-form health survey (SF-36). I. conceptual framework and item selection. *Med Care* 1992; 30: 473-83.
28. WHITCHER JP, SHIBOSKI CH, SHIBOSKI SC *et al*.: A simplified quantitative method for assessing keratoconjunctivitis sicca from the Sjögren's syndrome international registry. *Am J Ophthalmol* 2010; 149: 405-15.
29. DE VITA S, LORENZON G, ROSSI G, SABELLA M, FOSSALUZZA V: Salivary gland echography in primary and secondary Sjögren's syndrome. *Clin Rheumatol* 1992; 11: 385-7.
30. ZHANG S, ZHU J, ZHANG X, HE J, LI J: Assessment of the stiffness of major salivary glands in primary Sjögren's syndrome through quantitative acoustic radiation force impulse imaging. *Ultrasound Med Biol* 2016; 42: 645-53.
31. THOMAS A, WARM M, HOOPMANN M, DIEKMANN F, FISCHER T: Tissue Doppler and strain imaging for evaluating tissue elasticity of breast lesions. *Acad Radiol* 2007; 14: 522-9.
32. FISCHER T, PEISKER U, FIEDOR S *et al*.: Significant differentiation of focal breast lesions: raw data-based calculation of strain ratio. *Ultraschall Med* 2012; 33: 372-9.
33. DÖRNER T, BOWMAN SJ, FOX R *et al*.: Ianalumab (VAY736), a dual mode-of-action biologic combining BAFF receptor inhibition with B cell depletion, reaches primary endpoint for treatment of primary Sjögren's syndrome. *Ann Rheum Dis* 2020; 79 (Suppl. 1): 187-88.
34. GAZEAU P, CORNEC D, JOUSSE-JOULIN S, GUELLEC D, SARAUX A, DEVAUCHELLE-PENSEC V: Time-course of ultrasound abnormalities of major salivary glands in suspected Sjögren's syndrome. *Joint Bone Spine* 2018; 85: 227-32.
35. DEJACO C, DE ZORDO T, HEBER D *et al*.: Real-time sonoelastography of salivary glands for diagnosis and functional assessment of primary Sjögren's syndrome. *Ultrasound Med Biol* 2014; 40: 2759-67.
36. KNOPF A, HOFAUER B, THÜRMEL K *et al*.: Diagnostic utility of acoustic radiation force impulse (ARFI) imaging in primary Sjögren's syndrome. *Eur Radiol* 2015; 25: 3027-34.
37. KIMURA-HAYAMA E, CRIALES-VERA S, AZPEITIA-ESPINOSA L *et al*.: Elastographic ultrasound: an additional image tool in Sjögren's syndrome. *Int J Rheum Dis* 2018; 21: 1293-1300.
38. KNOPF A, MANSOUR N, CHAKER A, BAS M, STOCK K: Multimodal ultrasonographic characterization of parotid gland lesions – A pilot study. *Eur J Radiol* 2012; 81: 3300-05.
39. KLOTZ LV, INGRISCH M, EICHHORN ME *et al*.: Monitoring parotid gland tumors with a new perfusion software for contrast-enhanced ultrasound. *Clin Hemorheol Microcirc* 2014; 58: 261-9.
40. STRIETH S, SIEDEK V, RYTVINA M, GURKOV R, BERGHAUS A, CLEVERT D-A: Dynamic contrast-enhanced ultrasound for differential diagnosis of submandibular gland disease. *Eur Arch Otorhinolaryngol* 2014; 271: 163-9.
41. GIUSEPPETTI GM, ARGALIA G, SALERA D, RANALDI R, DANIELI G, CAPPELLI M: Ultrasounographic contrast-enhanced study of Sicca syndrome. *Eur J Radiol* 2005; 54: 225-32.
42. LUCIANO N, FERRO F, BOMBARDIERI S, BALDINI C: Advances in salivary gland ultrasonography in primary Sjögren's syndrome. *Clin Exp Rheumatol* 2018; 36 (Suppl. 114): S159-64.
43. DEVAUCHELLE-PENSEC V, GOTTENBERG J-E, JOUSSE-JOULIN S *et al*.: Which and how many patients should be included in randomized controlled trials to demonstrate the efficacy of biologics in primary Sjögren's syndrome? *PLoS One* 2015; 10: e0133907.